Effects of finite curvature on soliton dynamics in a chain of non-linear oscillators

2001 J. Phys.: Condens. Matter 13 1181

(http://iopscience.iop.org/0953-8984/13/6/301)

INSTITUTE OF PHYSICS PUBLISHING JOURNAL OF PHYSICS: CONDENSED MATTER

J. Phys.: Condens. Matter **13** (2001) 1181–1192 www.iop.org/Journals/cm PII: S0953-8984(01)18353-0

Effects of finite curvature on soliton dynamics in a chain of non-linear oscillators

Peter L Christiansen[1], **Yuri B Gaididei**[2] **and Serge F Mingaleev**[2]

[1] Department of Mathematical Modelling, The Technical University of Denmark, DK-2800 Lyngby, Denmark
[2] Bogolyubov Institute for Theoretical Physics, Kiev 03143, Ukraine

E-mail: plc@imm.dtu.dk (P L Christiansen)

Received 26 October 2000, in final form 30 November 2000

Abstract

We consider a curved chain of non-linear oscillators and show that the interplay of curvature and non-linearity leads to a number of qualitative effects. In particular, the energy of non-linear localized excitations centred on the bending decreases when curvature increases, i.e. bending manifests itself as a trap for excitations. Moreover, the potential of this trap is a *double-well* one, thus leading to a *symmetry-breaking* phenomenon: a symmetric stationary state may become unstable and transform into an energetically favourable asymmetric stationary state. The essentials of symmetry breaking are examined analytically for a simplified model. We also demonstrate a threshold character of the scattering process, i.e. transmission, trapping, or reflection of the moving non-linear excitation passing through the bending.

1. Introduction

Recently, determination of the dynamical properties of physical systems with non-trivial geometry has attracted a growing level of interest because of their wide applicability in various physical and biophysical problems. Examples include biological macromolecules, nanotubes, microtubules, vesicles, and electronic and photonic waveguide structures [1–6]; the gene transcription is usually accompanied by a local DNA bending [7–9]; the electronic properties of carbon nanotubes depend drastically on their chirality [10]; T-shape junctions were recently proposed [11] as nanoscale metal–semiconductor–metal contact devices; periodically spaced, curved optical waveguides were proposed for observation of optical Bloch oscillations [12].

The geometry manifests itself in particular in creation of linear quasi-bound states (see, e.g., [13, 14]). On the other hand, it is well known that the balance between non-linearity and dispersion leads to the existence of spatially localized soliton-like excitations. Taken together, these two localization mechanisms compete and one may expect the *interplay of geometry and non-linearity to lead to qualitatively new effects*.

An example of non-linearity-induced change of the geometry of the system can be found in reference [15] where the classical Heisenberg model on an infinite elastic cylinder was

considered. It was shown that a periodic topological spin soliton induces a periodic pinch of the cylindrical manifold. These results are applicable to microtubules and vesicles comprised of magnetic organic materials [16]. The stationary lasing of the modes in a microdisk was investigated in reference [17] where it was shown that non-linear whispering gallery modes exist in the microdisk above some finite pumping thresholds.

In this paper we consider a curved chain of non-linear oscillators which is described by the non-linear Schrödinger (NLS) model with the coupling coefficients depending on the distance between oscillators. This model has been in particular used as an approximation to the non-linear dynamics of biological macromolecules, such as proteins [18–20] and DNA [21]. It was shown that non-linear excitations should play a key part in the biological functioning of such molecular chains. However, usually they are investigated on the assumption that the chain has a straight rod-like configuration. On the other hand, the thermodynamical properties of these macromolecules cannot be understood without taking into account their flexibility and the existence of non-trivial spatial configurations. Moreover, there is increasing evidence that non-trivial spatial configurations should play a part in non-linear dynamics of the macromolecules. In particular, the DNA molecule is usually hooked [7–9] by the RNA-polymerase which binds to the promoter segment of DNA and then initiates the DNA transcription.

This raises the interesting question of whether a non-trivial spatial configuration of the chain could introduce some new qualitative effects into the non-linear dynamics of the system. In the present paper we demonstrate some of such effects on the example of the chain with a single parabolic bending. In section 2 we describe the model and present the results of numerical calculations of stationary excitations. In particular, we discuss the multi-stability phenomenon and curvature-induced symmetry breaking in the spectrum of non-linear excitations. In section 3 we analyse analytically a minimal model which gives qualitatively the same behaviour as the original model. In section 4 we consider dynamical properties of non-linear excitations, in particular scattering of the moving excitations by the chain bending. Section 5 presents the concluding discussion.

2. The system and equations of motion

The model that we study is described by the Hamiltonian

$$H = \sum_n \left\{ 2|\psi_n|^2 - \sum_{m \neq n} J_{n,m} \psi_n^* \psi_m - \frac{1}{2}|\psi_n|^4 \right\} \tag{1}$$

where $\psi_n(t)$ is the complex amplitude at the site n ($n = 0, \pm 1, \pm 2, \ldots$). For instance, in the case of the two-strand DNA model [22], ψ is the complex amplitude of the base-pair stretching vibration. We assume that the excitation transfer $J_{n,m}$ in the dispersive term depends on the distance in the embedding space between the sites n and m: $J_{n,m} \equiv J(|\vec{r}_n - \vec{r}_m|)$, where the radius vector $\vec{r}_n = (x_n, y_n, z_n)$ characterizes the spatial position of the site n. Of course, when $J_{n,m}$ models electromagnetic coupling between dipoles, this coefficient will depend also on the relative angles. However, in some cases such dependence is not present. For example, for the semiflexible ribbon polymers [23] the dipoles are orthogonal to the plane in which the chain can be curved, so the corresponding interaction would depend only on the distance between the dipoles.

From the Hamiltonian (1), we obtain the equation of motion in the form

$$\mathrm{i}\,\frac{\mathrm{d}}{\mathrm{d}t}\psi_n - 2\psi_n + \sum_{m \neq n} J_{n,m}\psi_m + |\psi_n|^2\psi_n = 0. \tag{2}$$

The Hamiltonian H and the number of excitations (quanta) $N = \sum_n |\psi_n|^2$ are both conserved quantities. The sites are assumed to be equidistantly placed on a planar envelope curve.

We consider the properties of non-linear excitations in the vicinity of the bends where the envelope curve can be modelled by a parabola (see the top part of figure 1): $y_n = \kappa x_n^2/2$ and $z_n = 0$ with κ being the inverse radius of curvature at the bending point. We assume that the chain is inextensible—that is, the distance between neighbouring sites is constant: $|\vec{r}_{n+1} - \vec{r}_n| = 1$ for all n and κ. Therefore, when κ is not too large ($|\vec{r}_m - \vec{r}_n| > 1$ for all $|n - m| > 1$) the excitation dynamics does not depend on the curvature of the system in the *nearest-neighbour approximation*, when $J_{n,m} = J\delta_{n-m,\pm 1}$.

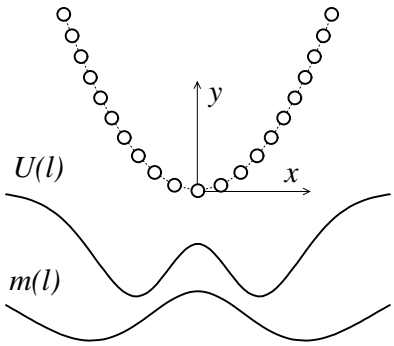

Figure 1. The curved chain under consideration and the corresponding effective double-well potential U and mass m, created by the bending.

In many physical problems, however, the nearest-neighbour approximation is too crude. For example, the effective dispersive interaction between non-linear layers in non-linear dielectric superlattices is exponential, $\exp(-\alpha r)$, with the inverse radius α depending on parameters of the lattice (superlattice spacing, linear refractive index, and so on) [24]. In the framework of the Peyrard–Bishop model [25,26] the non-linear dynamics of the DNA molecule can be described by equation (2) with the non-linear term of the opposite sign (because of the *repulsive* anharmonicity). In this case, ψ is the complex amplitude of the base-pair stretching vibration [22]. The base pairs (AT, GC) in the DNA molecule are usually asymmetric (see, e.g., [1]), and therefore the vibration which corresponds to the stretching of the hydrogen bonds connecting the two bases transfers along the chain due to the dipole–dipole interaction decaying with the distance r as $1/r^3$. Since the dipole moments of base pairs are almost perpendicular to the molecular axis [1], they are almost parallel to each other and the interaction between dipoles is also repulsive ($J_{n,m} < 0$). Thus, after substitutions $t \to -t$ and $J_{n,m} \to -J_{n,m}$, this model of the DNA molecule will be described by equation (2). We have investigated both cases, $J_{n,m} = J\exp(-\alpha|\vec{r}_n - \vec{r}_m|)$ and $J_{n,m} = J|\vec{r}_n - \vec{r}_m|^{-s}$, with qualitatively the same results. In this paper, however, we discuss only the first case in detail. It is known [27] that in the case of a straight rod-like chain ($\kappa = 0$) such an NLS model exhibits bistability in the spectrum of non-linear stationary states for $\alpha < 1.7$. To distinguish these effects from the finite-curvature effects we use $\alpha = 2$ in what follows.

For stationary states, $\psi_n(t) = \phi_n(\Lambda)e^{i\Lambda t}$, where Λ is the non-linear frequency and $\phi_n(\Lambda)$ is the excitation amplitude of the nth site, equation (2) reduces to the system of non-linear algebraic equations

$$\sum_{m\neq n} J_{nm}\phi_m + \phi_n^3 = (2 + \Lambda)\phi_n \tag{3}$$

which can be solved, for instance, by Newton–Raphson iterations.

In figure 2 we demonstrate that in the linear limit, i.e. when the term ϕ_n^3 in equation (3) is neglected, the bending creates at least one linear localized state. The profile of the first bound state, which is always present, is shown in figure 3(a). When the curvature of the chain increases, new localized states emerge from the continuum spectrum; their profiles are shown in figure 3. As has been recently proven for a similar system [28], the number of these bound states can exceed any positive integer provided that the chain is curved 'enough'.

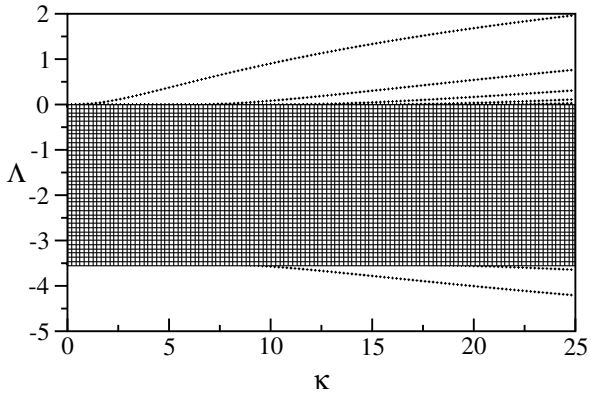

Figure 2. The dependence of the spectrum of linear excitations on the curvature of the chain for $\alpha = 2$ and $J = 6.4$. Localized linear bound states emerge above (symmetric states) and below (antisymmetric states) the continuum spectrum of extended states.

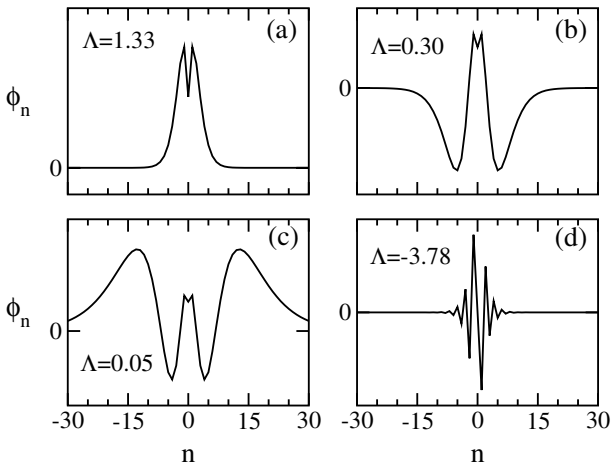

Figure 3. Profiles of the linear bound states from figure 2 for $\kappa = 15$.

However, in the present paper we shall study the case of smooth bendings for which only the first bound state is present. In figure 4 we plot the dependence of $N(\Lambda)$ obtained numerically for both the straight rod-like and the curved chains. As may be inferred from this figure, several new features arise as a consequence of the finite curvature.

Specifically, *there appears a gap* at small Λ in which no localized solution can exist. As can be seen from figure 2, this gap originates from the existence of the linear two-hump bound state discussed above.

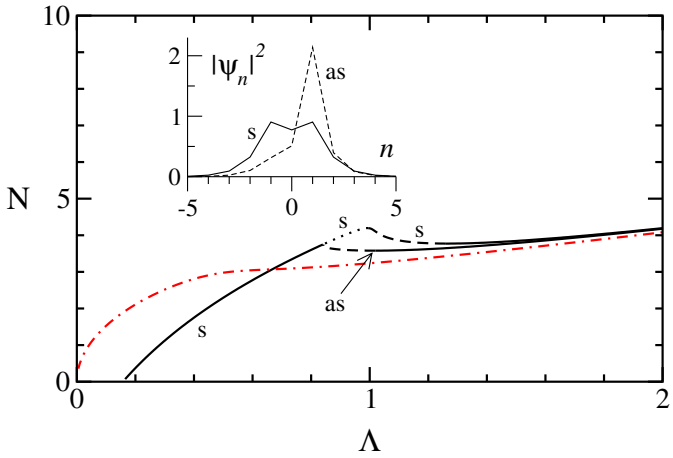

Figure 4. The number of excitations $N(\Lambda)$ for the straight chain ($\kappa = 0$; *dot–dashed line*) and curved chain ($\kappa = 3$; *solid lines* for stable states, *dashed lines* for the states unstable with respect to the breathing mode, and *dotted line* for the states unstable with respect to the Peierls mode) for $\alpha = 2$ and $J = 6.4$. In the inset, the shapes of the symmetric (s) and asymmetric (as) stationary states for $N = 3.6$ are shown.

In the case of the curved chain there are *two branches of stationary states*: a branch of symmetric localized excitations (s), which exists for all values of N, and a branch of *asymmetric localized excitations* (as), which exists only for $N > N_{th}(\kappa)$. The threshold value $N_{th}(\kappa)$ decreases when κ decreases and vanishes in the limit $\kappa \to 0$. The symmetric stationary state has a two-humped shape (evolved from the linear two-hump localized mode), while in the asymmetric state the maximum is shifted either to the left or to the right from the centre of symmetry $n = 0$ (see the inset in figure 4).

In contrast to the case of the straight rod-like chain (see the dot–dashed line in figure 4), the dependence $N(\Lambda)$ for the symmetric stationary states in a curved chain is *non-monotonic*. That is, there exists an interval of N in which three different symmetric states coexist for each excitation number; two of them are usually stable [27, 29]. Such a bistability phenomenon arises in the straight rod-like chain only for smaller values of $\alpha < 1.7$. Thus, one may conclude that the bending of the chain facilitates the *bistability of non-linear excitations*.

The energy of the symmetric as well as asymmetric localized states is a monotonically decreasing function of the curvature (see figure 5). Thus, one may expect that the *non-linear localized excitation may facilitate bending of a flexible molecular chain*. For $N > N_{th}(\kappa)$, when symmetric and asymmetric stationary states coexist, the *asymmetric state is always energetically more favourable*. Taking into account that in the linear limit the ground state of the model is symmetric with respect to the centre of symmetry $n = 0$, one can conclude that *combined action of the finite curvature and non-linearity provides the symmetry breaking* in the system.

In addition to the smooth bending, we studied the case of the wedge: $y_n = |x_n| \tan(\theta)$, and obtained qualitatively the same results. We checked also that the exact form of the dispersive interaction is not of serious concern here. To this end, we studied the case where the dispersive interaction has a power dependence on the distance:

$$J_{n,m} = J|\vec{r}_n - \vec{r}_m|^{-s}.$$

Qualitatively the same results were obtained for this case, too. The symmetry breaking which we observe means that there is a bistability in the spectrum of non-linear excitations: the

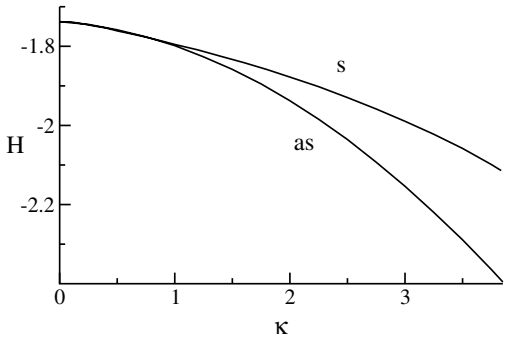

Figure 5. The energy of symmetric (s) and asymmetric (as) non-linear excitations versus the curvature κ for $\alpha = 2$, $J = 6.4$, and $N = 4$.

excitation can be localized either to the left or to the right of the bending. By applying an external periodic field one can achieve switching between these two states. In this way we may expect a new resonance to appear in the response of the system to a periodic driving.

3. The analytical approach and minimal model

To gain a better insight into the symmetry-breaking mechanism, let us consider the continuum limit of the discrete NLS model given by equations (1) and (2). We are interested here in the case where the characteristic size of the excitation is much larger than the lattice spacing. This permits us to replace $\psi_n(t)$ by the function $\psi(\ell, t)$ of the arc-length ℓ which is the continuum analogue of n. Using the Euler–Maclaurin summation formula [30] we get

$$H = \int_{-\infty}^{\infty} \left\{ \frac{1}{2m(\ell)} \left| \frac{\partial \psi}{\partial \ell} \right|^2 + U(\ell)|\psi|^2 - \frac{1}{2}|\psi|^4 \right\} \mathrm{d}\ell. \tag{4}$$

Here,

$$m^{-1}(\ell) = \int_{-\infty}^{\infty} (\ell' - \ell)^2 J_{\ell,\ell'} \, \mathrm{d}\ell'$$

is the inverse effective mass of the excitation, and

$$U(\ell) = -\int_{-\infty}^{\infty} J_{\ell,\ell'} \, \mathrm{d}\ell'$$

is the energy shift due to the dispersive interaction. Near the bending point the number of neighbours available for excitation is larger than far away where the curvature is small. Near the bending the effective potential, $U(\ell)$, exhibits a double-well shape. This, together with the resulting double-well spatial dependence of the effective mass $m(\ell)$, is why the excitation is localized. The attractive potential $U(\ell)$ consists of two symmetric wells whose positions ($\pm a$) and depths ($\Delta \equiv U(|\ell| \to \infty) - U(a)$) are determined by the range of the dispersive interaction and the peculiarities of the bending geometry (see figure 1). For example, in the case of the wedge, $y_n = |x_n| \tan(\theta)$, we get for $\theta < \pi/4$

$$U(\ell) = -\frac{J}{\alpha}(2 - \mathrm{e}^{-\alpha|\ell|}) - \frac{J}{\alpha} \begin{cases} \mathrm{e}^{-\alpha|\ell|\cos(2\theta)} & \text{when } \theta < 1/2 \\ \alpha|\ell| K_1(\alpha|\ell|) & \text{when } \theta \to \pi/4 \end{cases}$$

where $K_n(z)$ denotes the modified Bessel function [30]. The distance between the potential minima $2a \approx (1 + \theta^2)/\alpha$ and their depth $\Delta \approx 4eJ\theta^2/\alpha$ increase when the wedge angle

$\theta \to \pi/4$. Note that a Hamiltonian similar to equation (4) with $U(\ell) \equiv 0$ was introduced in reference [31] to study the effects of the DNA bending on breather trapping. A step-function dependence of the effective mass $m(\ell)$ was assumed there.

The NLS model (4) is still very difficult to solve analytically. But it is interesting anyway to find a model—chosen as simple as possible—which gives qualitatively the same results as the original model. Such a model can be obtained by using the stepwise approximation

$$U(\ell) = -\frac{2J}{\alpha} - \Delta \sum_{\sigma=\pm} (H(\ell - \sigma a + w/2) - H(\ell - \sigma a - w/2)) \tag{5}$$

where $H(x)$ is the Heaviside step function, w is the width of the potential well. A similar expression can be written for the effective mass $m(\ell)$. In the stepwise approach the stationary equation which corresponds to the Hamiltonian (4) can be solved and the corresponding eigenvalue problem can be explored. However, results obtained in this manner look very cumbersome. Therefore we shall make a further simplification by applying the limit $w \to 0$, keeping the product $w\Delta \equiv \epsilon$ constant in equation (5). In this way we arrive at the following minimal model:

$$\mathrm{i}\frac{\partial \psi}{\partial t} + \frac{\partial^2 \psi}{\partial \ell^2} + \epsilon(\delta(\ell - a) + \delta(\ell + a))\psi + |\psi|^2\psi = 0 \tag{6}$$

where the gauge transformation $\psi \to \psi \exp(-\mathrm{i}\, 2Jt/\alpha)$ was used. Introducing into equation (6) the stationary-state *ansatz* $\psi(\ell, t) = \phi(\ell)\exp(\mathrm{i}\Lambda)$ where $\phi(\ell) \to 0$ when $|\ell| \to \infty$, we find that

$$\phi(\ell) = \begin{cases} \sqrt{2\Lambda}\,\mathrm{sech}(\sqrt{\Lambda}(\ell - \ell_{-1})) & \text{when } \ell < -a \\ \sqrt{\dfrac{2\Lambda(1-m)}{2-m}}\,\mathrm{nd}\left(\sqrt{\dfrac{\Lambda}{2-m}}(\ell - \ell_0)|m\right) & \text{when } |\ell| < a \\ \sqrt{2\Lambda}\,\mathrm{sech}(\sqrt{\Lambda}(\ell - \ell_1)) & \text{when } \ell > a \end{cases}$$

where $\mathrm{pq}(u|m)$ (p, q = c, s, d, n) are the Jacobi elliptic functions with the modulus m [30]. The parameters $\ell_{\pm 1}$, ℓ_0, and m are determined from the relations

$$\begin{aligned} &\mathrm{sech}(\sqrt{\Lambda}(a \mp \ell_{\pm 1})) = \sqrt{\frac{1-m}{2-m}}\,\mathrm{nd}\left(\sqrt{\frac{\Lambda}{2-m}}(a \mp \ell_0|m)\right) \\ &F(\ell_0, m) \equiv \sqrt{1 - m(1-m)\,\mathrm{sd}^2(u_+|m)} + m\,\mathrm{sd}(u_+|m)\,\mathrm{cn}(u_+|m) \\ &\qquad - \sqrt{1 - m(1-m)\,\mathrm{sd}^2(u_-|m)} + m\,\mathrm{sd}(u_-|m)\,\mathrm{cn}(u_-|m) = 0 \\ &\sqrt{1 - m(1-m)\,\mathrm{sd}^2(u_\pm|m)} + m\,\mathrm{sd}(u_\pm|m)\,\mathrm{cn}(u_\pm|m) = \sqrt{\frac{2-m}{\Lambda}}\epsilon \end{aligned} \tag{7}$$

where

$$u_\pm = \sqrt{\Lambda/(2-m)}(a \pm \ell_0).$$

Using the above expressions one can evaluate the number of excitations which correspond to the stationary solution

$$N = 4(\sqrt{\Lambda} - \epsilon) + 2\sqrt{\frac{\Lambda}{2-m}} \sum_{\sigma=\pm 1} E(\mathrm{am}(u_\sigma)|m) \tag{8}$$

where $\mathrm{am}(u)$ is the amplitude and $E(\phi|m)$ is the elliptic integral of the second kind [30].

The equation $F(\ell_0, m) = 0$ always has a solution $\ell_0 = 0$. This corresponds to the symmetric two-hump wave function $\phi(\ell)$. In addition, $\ell_0 \neq 0$ solutions appear for $\Lambda \geqslant \Lambda_c$

with the threshold value Λ_c being determined from the condition $\partial F/\partial \ell_0 = 0$ for $\ell_0 = 0$. In other words, a symmetry-breaking bifurcation to a doubly degenerate branch of asymmetric solutions occurs at the point $\Lambda = \Lambda_c$. It follows from equation (7) that the symmetry-breaking bifurcation is determined by the equation

$$(1 - 2\,\mathrm{sn}^2 + m\,\mathrm{sn}^4)\sqrt{1 - 2m\,\mathrm{sn}^2 + m^2\,\mathrm{sn}^2} = (1 - m)\,\mathrm{sn}\,\mathrm{cn}$$

with

$$\mathrm{sn} \equiv \mathrm{sn}(\sqrt{\Lambda/(2 - m)}|m).$$

The results of the analytical consideration of the non-linear eigenvalue problem based on equations (7) and (8) are shown in figure 6. As in the original model, the stationary state (s) is unique and symmetric for small numbers of quanta N. But when the number of quanta exceeds some critical value there are two stationary states: symmetric (s) and asymmetric (as), with the asymmetric state being energetically favourable. Thus, similarly to the original model, the minimal model demonstrates a symmetry-breaking effect (localization in one of the wells). It is worth noting that a closely related phenomenon was observed in reference [32] where non-linear electromagnetic waves in a symmetric planar waveguide were studied. But in contrast to our case, the non-linear Schrödinger model with a stepwise non-linearity was considered.

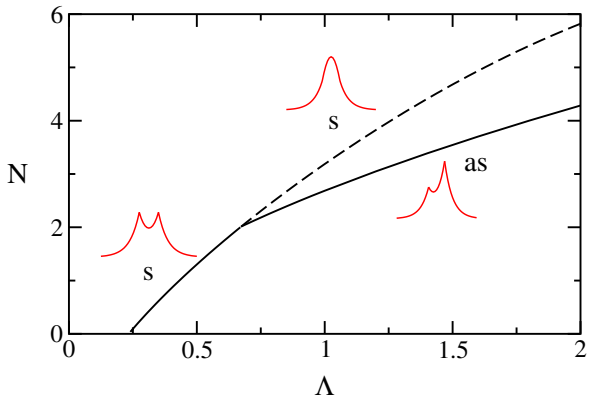

Figure 6. The dependence $N(\Lambda)$ for symmetric (s) and asymmetric (as) non-linear excitations in the two-impurity minimal model (6) with $\epsilon = 0.7$ and $a = 1$.

4. Dynamical properties of excitations

The dynamical properties of non-linear excitations include both the behaviour of immobile stationary excitations when they lose stability, and a scattering of the moving excitations by the bending.

The first issue has been considered in detail in reference [33] where we have shown that the symmetric two-humped stationary state can lose stability in two ways: due to softening of the antisymmetric Peierls internal mode and due to softening of the symmetric breathing mode. A typical evolution of the symmetric stationary state in the case when it becomes unstable with respect to the Peierls mode is shown in figure 7. One can see that the two-humped initial symmetric state evolves into an asymmetric state with an excited breathing internal mode.

In this paper we consider in more detail another item which is very intriguing from the viewpoint of possible applications: the scattering of moving excitations in their passage

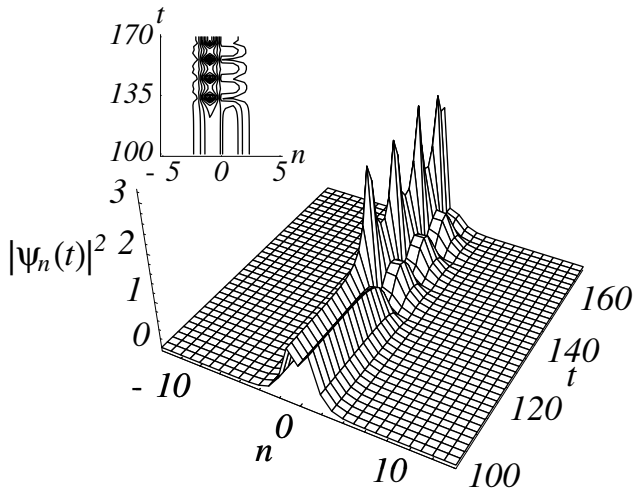

Figure 7. Switching from the symmetric state to the asymmetric state at $\alpha = 2$, $J = 6.4$, $\kappa = 4$, and $N = 3.96$.

through the centre of the bending. To accomplish this, we first obtained a stationary moving excitation by pushing (i.e. taking $\psi_n(0) = \phi_n(\Lambda)e^{ikn}$ with some k and Λ) the initially unmoving stationary state ϕ_n found numerically for the straight chain as described in section 2. Eventually, evolving over the course of 5000 time units, the excitation reached an almost stationary form. Substituting it into the curved chain far away from the bending, we found that the destiny of the excitation in passing though the bending region is strongly dependent on the curvature κ of the chain.

In figure 8 we plot the eventual velocity $v_{sc}(\kappa)$ of the excitation with $N = 2.39$ and initial velocity $v = 0.37$. One can see that for small κ ($\kappa < 0.2$) the bending practically does not change the excitation velocity. However, for $0.2 < \kappa < 1.07$ the transmission becomes clearly inelastic, leading to a decreasing of the excitation velocity. The excitation passes the bending region, leaving behind a part of its energy for exciting of the linear bound state (see figure 9(a)).

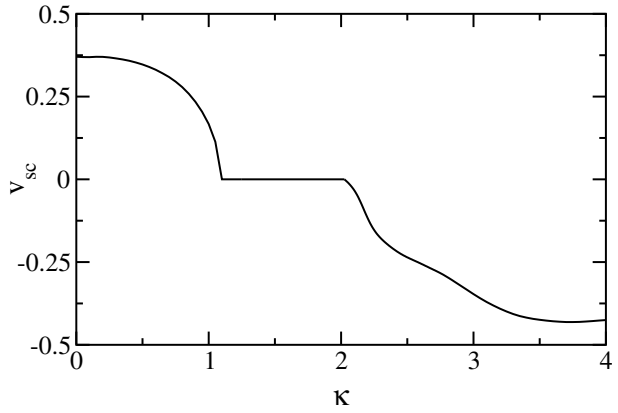

Figure 8. The velocity v_{sc} of the moving part of the excitation after the passage of the centre of the parabolic chain versus the curvature κ. Here $\alpha = 2$, $J = 6.4$, $N = 2.39$, and initial velocity $v = 0.37$.

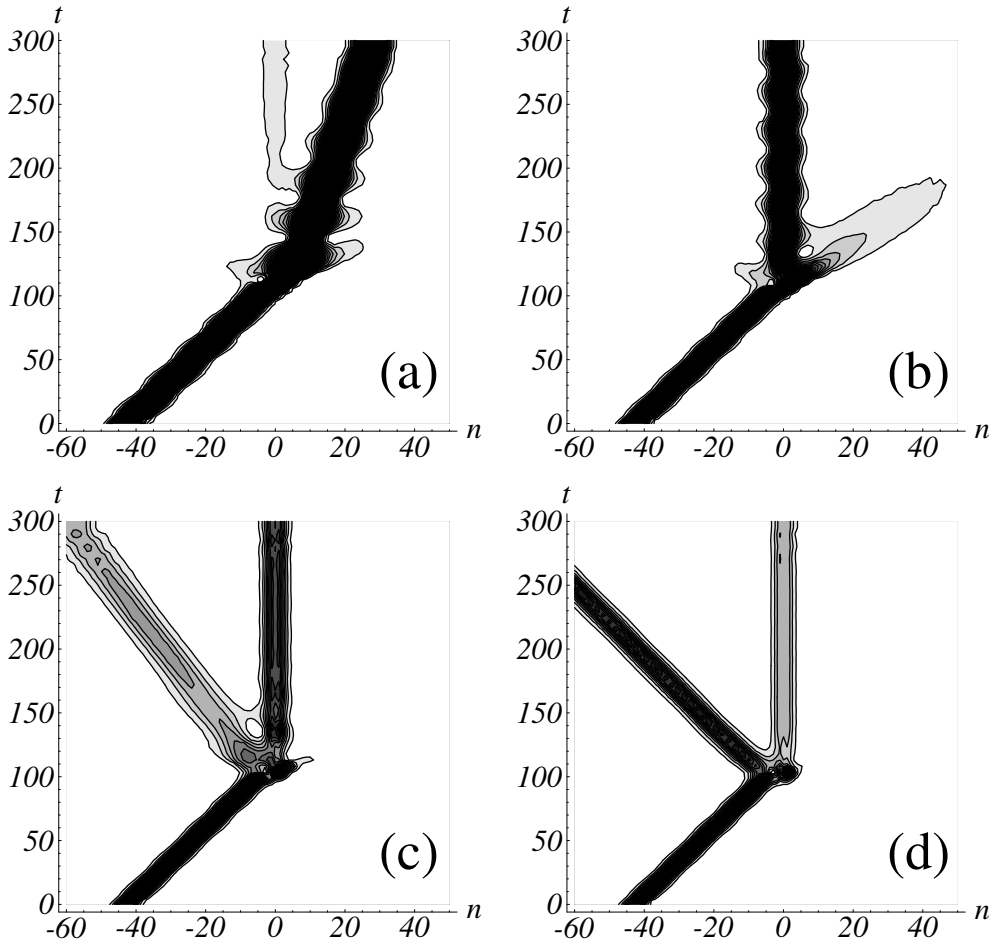

Figure 9. A density plot of $|\psi_n(t)|^2$ which demonstrates the scattering of the moving excitation from figure 8 for different values of κ: (a) 1.05, (b) 1.5, (c) 2.5, and (d) 3.0.

In the interval $1.07 < \kappa < 2.1$ the excitation is captured by the bending (see figure 9(b)), so in this case the bending clearly manifests itself as an effective trap. A similar phenomenon has been previously considered [31] as an effective breather-trapping mechanism for DNA transcription in the case of curved DNA. However, in reference [31] the bending has been accounted for effectively, by postulating some modification of the coupling constants around it.

Finally, for $2.1 < \kappa < 2.6$ the excitation is reflected from the bending; however, a significant part of the initial excitation energy remains captured near the bending region (see figure 9(c)). In contrast, for $\kappa > 2.6$ the main part of the excitation energy is reflected from the bending and only a small part is captured (see figure 9(d)).

5. Conclusions

In conclusion, we have shown that the interplay of curvature and non-linearity in the chain of non-linear oscillators can lead to qualitative effects, such as symmetry breaking of the non-linear excitations and their trapping by the bending. We have demonstrated that the energy

of non-linear excitations decreases with the increasing of curvature of the chain and thus one can expect that the presence of non-linear localized excitation in the chain may facilitate its bending, if the chain is flexible enough.

These effects are tolerant of the choice of the coupling coefficients J_{nm}. In particular, qualitatively the same properties were obtained for the case of the dipole–dipole dispersive interaction with $J_{nm} = |\vec{r}_n - \vec{r}_m|^{-3}$. Specifically, in the case of the Davydov–Scott model [18, 19] with the dipole–dipole coupling between sites [20], for the parameters which characterize the motion of the amide-I excitation in proteins (they correspond to $N = 0.64$ in our model), decreasing of the ground-state energy due to a trapping by the bending with $\kappa = 1$ ($\kappa = 3$) comprises 10% (46%) of the whole excitation energy. This may also be important for the dynamics of DNA molecules and in particular for DNA melting where, in accordance with the Peyrard–Bishop model [25, 26], the non-linear properties of base-pair vibrations play a crucial role.

Acknowledgments

We thank A C Scott and M Peyrard for helpful discussions. YuBG and SFM would like to express their thanks to the Department of Mathematical Modelling, Technical University of Denmark, where the major part of this work was done. SFM acknowledges support from the European Commission RTN project LOCNET (HPRN-CT-1999-00163).

References

[1] Saenger W 1984 *Principles of Nucleic Acid Structure* (Berlin: Springer)
[2] Iijima S 1991 *Nature* **354** 56
[3] Bar-Ziv R and Moses E 1994 *Phys. Rev. Lett.* **73** 1392
Nelson P, Powers T and Seifert U 1995 *Phys. Rev. Lett.* **74** 3384
[4] Meunier J, Langevin D and Boccara N (ed) 1987 *Physics of Amphiphilic Layers* (Berlin: Springer)
[5] Imry Y 1997 *Introduction to Mesoscopic Physics* (New York: Oxford University Press)
[6] Soukoulis C M (ed) 1993 *Photonic Band Gaps and Localization* (New York: Plenum)
[7] Reiss C 1995 *Nonlinear Excitations in Biomolecules* ed M Peyrard (Berlin–Les Ulis: Springer–Les Editions de Physique) p 29
[8] Heumann H, Ricchetti M and Werel W 1988 *EMBO J.* **7** 4379
[9] Burley S K 1994 *Nature Struct. Biol.* **1** 638
Kim J L, Nikolov D B and Burley S K 1993 *Nature* **365** 520
[10] Hamada N, Sawada S and Oshiyama A 1992 *Phys. Rev. Lett.* **68** 1579
[11] Menon M and Srivastava D 1997 *Phys. Rev. Lett.* **79** 4453
[12] Lenz G, Talanina I and de Sterke C M 1999 *Phys. Rev. Lett.* **83** 963
[13] Kirczenow G 1989 *Phys. Rev.* B **39** 10 452
[14] Gaididei Yu B, Malysheva L I and Onipko A I 1992 *J. Phys.: Condens. Matter* **4** 7103
[15] Dandoloff R, Villain-Guillot S, Saxena A and Bishop A R 1995 *Phys. Rev. Lett.* **74** 813
Saxena A and Dandoloff R 1997 *Phys. Rev.* B **55** 11049
[16] Saxena A, Dandoloff R and Lookman T 1998 *Physica* A **261** 13
[17] Harayama T, Davis P and Ikeda K S 1999 *Phys. Rev. Lett.* **82** 3803
[18] Davydov A S 1985 *Solitons in Molecular Systems* (Dordrecht: Reidel)
[19] Scott A C 1992 *Phys. Rep.* **217** 1
[20] Cruzeiro-Hansson L 1998 *Phys. Lett.* A **249** 465
[21] Yakushevich L V 1998 *Nonlinear Physics of DNA* (New York: Wiley)
[22] Gaididei Yu B, Mingaleev S F, Christiansen P L, Johansson M and Rasmussen K Ø 1998 *Nonlinear Cooperative Phenomena in Biological Systems* ed L Mattson (Singapore: World Scientific) p 176
[23] Golestanian R and Liverpool T B 2000 *Phys. Rev.* E **62** 5488
[24] Gaididei Yu B, Christiansen P L, Rasmussen K Ø and Johansson M 1997 *Phys. Rev.* B **55** R13 365
[25] Peyrard M and Bishop A R 1981 *Phys. Rev. Lett.* **62** 2755
[26] Dauxois T, Peyrard M and Bishop A R 1993 *Phys. Rev.* E **47** 684

[27] Johansson M, Gaididei Yu B, Christiansen P L and Rasmussen K Ø 1998 *Phys. Rev.* E **57** 4739
[28] Exner P 2000 Bound states of infinite curved polymer chains *Preprint* arXiv:math-ph/0010046
[29] Gaididei Yu B, Mingaleev S F, Christiansen P L and Rasmussen K Ø 1997 *Phys. Rev.* E **55** 6141
[30] Abramowitz M and Stegun I 1972 *Handbook of Mathematical Functions* (New York: Dover)
[31] Ting J J-L and Peyrard M 1996 *Phys. Rev.* E **53** 1011
[32] Akhmediev N N 1982 *Zh. Eksp. Teor. Fiz.* **83** 545 (Engl. Transl. 1982 *Sov. Phys.–JETP* **56** 299)
[33] Gaididei Yu B, Mingaleev S F and Christiansen P L 2000 *Phys. Rev.* E **62** R53
[34] Mingaleev S F, Christiansen P L, Gaididei Yu B, Johansson M and Rasmussen K Ø 1999 *J. Biol. Phys.* **25** 41